Contributions to Mineralogy and Petrology (2021) 176:13
https://doi.org/10.1007/s00410-020-01764-3

ORIGINAL PAPER

# Chemical and textural diversity of Kameni (Greece) dacites: role of vesiculation in juvenile and mature basal crystal masses

**Michael D. Higgins[1] · Anouk Debecq[2] · Jacqueline Vander Auwera[3] · Paraskevi Nomikou[4]**

Received: 25 August 2020 / Accepted: 12 December 2020 / Published online: 28 January 2021


## Abstract

Dacite lavas erupted from Kameni Islands volcanic centre (Greece) during the last 2000 years have a limited range in chemical composition ($SiO_2$ = 64.0–68.5%) which contrasts with their wide range in plagioclase abundance (3–22%) and crystal size distributions. Most plagioclase crystals have simple zoning and occur independently or in loose clusters with finer-grained cores. We propose that magmatic diversity was produced by the interaction between crystals that formed at the base of a magma reservoir and bubbles produced by injection and vesiculation of more mafic magma. Two end-member situations can be identified: in juvenile systems, the basal crystal mass is loosely connected and readily disrupted by bubble formation. The crystal–bubble couples accumulate at the top of the reservoir, from where they can enter the sub-volcanic plumbing system to produce high-crystal content, chemically unevolved magmas. In the mature system, the crystal mass is well connected so bubbles displace the evolved, interstitial magma and liberate only a smaller number of crystals from the crystal mass. This process produces chemically evolved magmas, with lower crystal contents. The oldest lavas seem to have been produced from mature systems, whereas the youngest eruptions were of lavas produced from juvenile systems. This progression may reflect an overall reduction in repose times during the last 2000 years.

**Keywords** Dacite · Enclaves · Bubbles · Texture · CSD · Santorini

## Introduction

An important challenge in the study of volcanos is to understand how the underlying magmatic system has evolved with time, and how it will behave in the future. For recent eruptions or intrusive events, we can use geological observation, cultural information, and geophysical methods to determine the timing and movements of magma (Pyle 2017). Aspects of current magma distribution can be measured using seismic tomography (Hooft et al. 2019; McVey et al. 2019). However, many older eruptions can only be understood by studying lava and ash produced by the eruptions.

An ideal volcano for such a study would be easily accessible, would erupt frequently with well-described and timed volcanic events, and volcanic products would be well preserved. The Kameni Islands volcanic centre has many of these characteristics and has hence been the object of many studies to be described later. Most work to date has examined the chemical composition of the lavas and enclaves, with a much smaller number of studies on the texture (microstructure) of the rocks. However, few have used the combination of geochemical and textural work that has proved to be so powerful in the understanding of other active volcanos (e.g. Higgins et al. 2015).

Here we want to address the following problems: how was the textural and chemical diversity of the Kameni dacites produced and what were the mechanisms in the underlying magmatic system that produced this diversity; can the eruptions of the Kameni Islands during the last 2000 years

Communicated by Timothy L. Grove.

**Supplementary Information** The online version contains supplementary material available at https://doi.org/10.1007/s00410-020-01764-3.

✉ Michael D. Higgins
mhiggins@uqac.ca

[1] Sciences Appliquées, Université du Québec à Chicoutimi, Québec G7J 4M2, Canada

[2] Université Libre de Bruxelles, Bruxelles, Belgium

[3] Université de Liège, Liège, Belgium

[4] National and Kapodistrian University of Athens, Athens, Greece

be considered as a single, stable phase, or must the history be divided up into several separate volcanic cycles? This leads us to consider if we are now near the end of an eruptive cycle and how this may inform us about the nature of future eruptions.

We would like to mention that although magma reservoirs are discussed in the text and figures we acknowledge that the magmatic 'plumbing system' under the Kameni volcanos is much more complex than this, as shown by the recent seismic unrest and tomographic models (Hooft et al. 2019; McVey et al. 2019; Parks et al. 2012).

## The Kameni islands

### Eruptive history

Santorini volcano (also known as Thira or Thera) was formed at least 650,000 years ago and has had numerous major Plinian eruptions (Druitt et al. 2019b). The most recent was the 'Minoan' eruption in ~ 1600 BCE which produced a caldera that forms the central bay between Thira and Thirasia islands (Druitt et al. 2019a). Since that time, eruptions have been confined to the central part of the caldera. We do not know when extrusive activity restarted, but the earliest subaerial post-Minoan eruption was in 197 BCE and produced the island of Hiera (Theodorakopoulou et al. 2020). It was probably situated 4 km southwest of Fira town and reduced to a bank before being buried by the 1866–70 eruption (Fig. 1). The next subaerial eruption was in 46–47 CE and produced the core of Palea Kameni Island (PK). The eruptive products extend underwater to the south and west. The 726 CE subaerial eruption was the most violent in the history of the islands (VEI = 4) and caused considerable damage (Vougioukalakis and Fytikas 2005). It produced large quantities of pumice which floated as far as the Dardanelles and may have been used to justify the imposition of the Iconoclasm by the Byzantine Emperor Leo III. Although knowledge of underwater eruptions is sparse, there may have been a hiatus for over 800 years until 1570 CE when subaerial activity restarted 3 km to the northeast. Although the current outcrop of this flow is small the flow appears to continue underwater for 2 km to the north. Large effusive eruptions continued to occur at decreasing intervals building Nea Kameni Island (NK). The volume of the subaerial flows diminished in the twentieth century and the last event in 1950 CE was very small.

Recent high-resolution bathymetric observations have considerably expanded our view of the subaerial flows, showing them to be significantly larger than previously estimated. In addition, the studies have revealed at least three submarine flows unrelated to the subaerial flows: NK North, NK East, and Drakon (Fig. 1; Nomikou et al. 2014). The eruption dates of these flows are partly constrained by historic lead-line bathymetry (Watts et al. 2015) and their relationships to adjacent flows: NK North erupted sometime

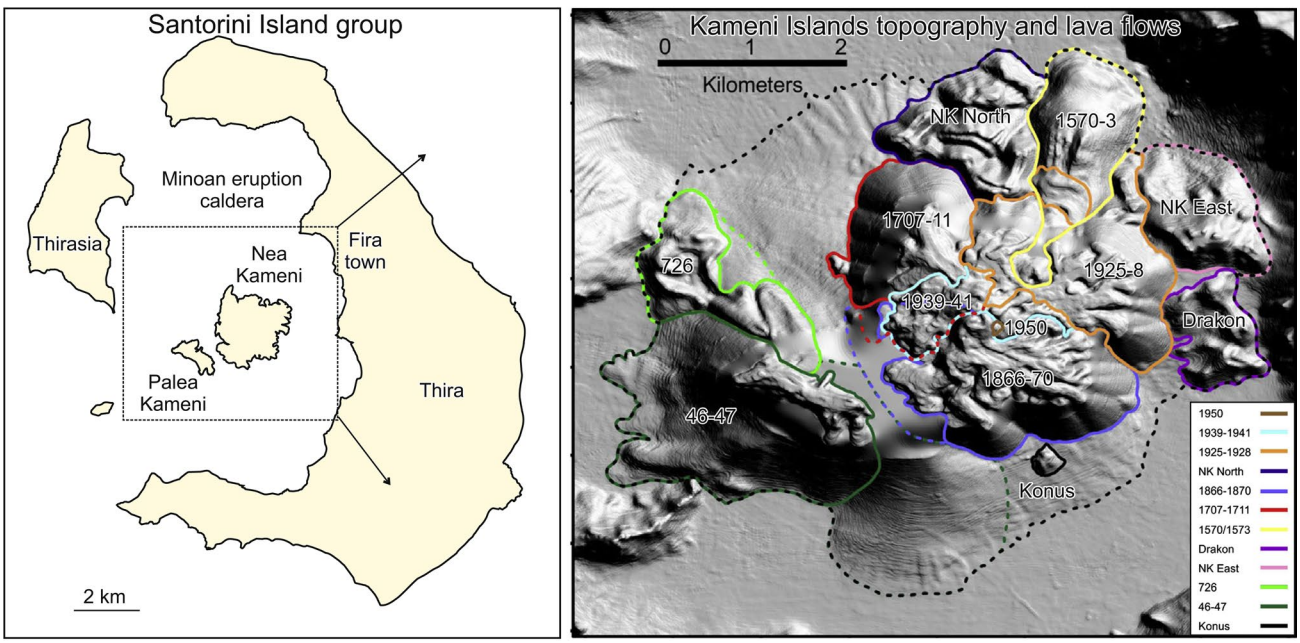


**Fig. 1** The Santorini Island group includes Thira (Thera), Thirasia as well as the Kameni islands whose lava flows are studied here. High-resolution bathymetry/topography of the Kameni group shows the underwater continuity of subaerial flows and the presence of some previously unknown flows. Source: (Nomikou et al. 2014)

between 1848 and 1925; Drakon erupted after 1848, and NK East erupted before 1848.

Seismic unrest in 2011–2012 was related to magma movements beneath the edifice (Newman et al. 2012; Parks et al. 2012, 2015). Earthquake loci showed that the magma rose along the southern caldera fault, essentially beneath the Kameni Islands, and stalled at a depth of about 4 km (Parks et al. 2015). This depth accords with seismic tomography models (Hooft et al. 2019; McVey et al. 2019). The magma then appeared to feed a sill beneath the caldera a few 100 m north of Nea Kameni, close to the centre of the northern part of the bay. Inflation indicated that about 1–2.$10^7$ $m^3$ of new magma was emplaced during the event (Parks et al. 2015). Helium isotopes suggest that the event was triggered by the injection of primitive magma (Rizzo et al. 2015).

The eruptive history of the currently accessible parts of the Kameni Island volcanic system appears to comprise two or three distinct phases. The first phase produced Palea Kameni island and culminated in the major explosive eruption of 726 CE. There was a hiatus for 800 years before activity resumed 3 km to the northeast and built Nea Kameni island. Chemical and textural data support this division into PK and NK phases, and also a less well-defined phase that comprises the latest eruptions (1939–1950). It is not clear if the 197 BCE eruption was part of the PK phase as we do not know its exact position or composition.

#### Relevant earlier work

The Kameni islands' lava flows, and their enclaves, have been the subject of several geochemical and textural studies over the last 30 years, commonly as part of a wider study on the whole Santorini volcanic system. The subaerial Kameni volcanic ensemble has many advantages: it is accessible, the rocks are mostly fresh, and all the flows are well dated. Samples of some of the underwater phases of the Kameni volcanic ensemble have recently become available (Nomikou et al. 2014).

The earliest study of the geochemistry of Santorini volcano was by Nicholls (1971), who examined a few Kameni samples. However, analyses mostly used uncorrected XRF and hence cannot be compared with more recent data. The first study using modern XRF methods was that of Huijsmans (1985). Some of his data was published in (Barton and Huijsmans 1986). Most of the analyses were of dacite samples and they concluded that despite a range in composition between individual samples, the mean chemical composition of flows changed little during the last 2000 years. Crystal size distributions (CSD) of plagioclase were determined in 10 samples of dacite by Higgins (1996b). These samples make up some of the material reanalysed in this study. Francalanci et al. (1998) analysed a large number of samples of dacite and enclaves but only published mean compositional values for each flow and a few representative analyses of enclaves. Zellmer et al. (2000) analysed dacites and enclaves as part of an isotopic study. Martin et al. (2006) included two analyses of dacite as part of a study of the enclaves. The overall conclusion of these studies is that the chemical composition of the dacites is relatively uniform, as compared to products of the Santorini volcano as a whole, but that there is enough geochemical variation to be studied by modern analytical techniques. However, textural variations are more pronounced than geochemical variations and the two together can help us understand the evolution of this magma system.

The enclaves in the dacite lavas have been studied as part of larger studies and independently. Most studies have looked at the overall chemical composition of the enclaves and concluded that their chemical composition is much more variable than that of the dacites (Barton and Huijsmans 1986; Francalanci et al. 1998; Martin 2005; Martin et al. 2006; Zellmer et al. 2000). The enclaves' textures in post-1925 flows were studied by Martin et al. (2006) who classified the enclaves into three groups of micrographic enclaves (A-1, A-2, B) and one group of cumulate enclaves. The latter is made of plagioclase crystals up to 10 mm long, frequently intergrown with olivine: they crystallised from mafic magma and been coarsened by equilibration at high temperatures. There are no data on the overall chemical composition of the cumulates. Finally, it should be noted that the enclaves are vesicular with a much higher bubble content than their surrounding magma (Martin 2005; Martin et al. 2006).

Different populations of plagioclase crystals have been recognised in the Kameni lavas, as in most andesites and dacites elsewhere. Plagioclase populations in enclaves have not been considered. Barton and Huijsmans (1986) identified 'phenocrysts' and 'xenocrysts' based on their composition and zoning. Their phenocrysts are euhedral, up to 1 mm long, with brown glass inclusions and compositions of $An_{55}$–$An_{42}$. The xenocrysts are generally larger, with resorbed anorthitic cores ($An_{90}$–$An_{71}$), and are considered to be derived from disaggregated enclaves. Stamatelopoulou-Seymour et al. (1990) studied the composition of a small number of crystals in much detail. They produced a similar classification but divided the first class of Barton and Huijsmans (1986) into inherited crystals and those that crystallised in situ. The abundance of these crystal populations was not discussed in either study.

## Methods

### Sampling

Samples were taken from the surface of the lava flows on Palea Kameni and Nea Kameni islands during two

campaigns in 1990 (Higgins 1996b) and 2017 (see supplementary table 1). All samples were fresh and unaltered. Dacite lava samples were selected to exclude visible enclaves, and enclaves were sampled avoiding contamination by dacite. We did not sample material from the scoria cones. The flow dates were determined from existing studies and field observations (Druitt et al. 1999).

The surface samples were complemented by samples taken underwater using an ROV (Sigurdsson et al. 2006). Most lava samples were fresh, but scoria samples appeared to have been altered by long exposure to seawater. We used the flow association and nomenclature of Nomikou et al. (2014). All the underwater lava samples were assigned to the NK North flow. Scoria samples were taken from the underwater surface of the 46–7 and 726 eruptions.

## Chemistry

The samples were coarsely crushed with a hammer and ground in an agate planetary mill to a fine powder. Major elements were analysed by X-ray fluorescence at the Université de Liège (Belgium) using a Thermofisher PERFORM'X X-ray fluorescence spectrometer with a Rh tube. These elements were measured on fused glass discs that were prepared with lithium tetra- and meta-borate and 0.35 g of rock powder previously dried at 1000 C for two hours. Some trace elements were also measured by X-ray fluorescence on pressed powdered pellets. The instrument was calibrated using 40–60 international standards for major and trace elements, respectively. Iron was expressed as $Fe_2O_3$. Reproducibility was estimated to be better than 1% for most major elements and 3% for minor elements. Most trace elements were analysed by ICP-MS following alkali fusion using a Thermo Scientific X-Series 2 with a collision cell (MRAC Tervuren, Belgium). Reproducibility was estimated to be better than 3%. Chemical data are presented in electronic appendix table S1.

## Petrography

Plagioclase textures were examined in polished thin sections using conventional transmitted light microscopy and cathodoluminescence (Fig. 2). The intensity and colour of the light emitted during cathodoluminescence are dominantly controlled by trace chemical composition (Pagel et al. 2000). The most important activator in plagioclase is $Mn^{2+}$, but $Cu^{2+}$, $Fe^{3+}$, $Ti^{4+}$, $Ce^{3+}$ and $Eu^{2+}$ may also be important (Mora and Ramseyer 1992). Another factor is lattice orientation, hence, twinning is commonly visible.

In this study, cathodoluminescence colour was used not only to help quantify plagioclase textures but also to identify the abundance of different petrographic classes of plagioclase (Götze et al. 2012; Higgins et al. 2015). The cathodoluminescence images were obtained using a CITL CL8200 cold-cathode instrument mounted on a regular petrographic microscope. Multiple images were mosaicked to give composite images that typically covered half a regular thin section. The texture of the plagioclase crystal population was quantified from the composite cathodoluminescence image. The cathodoluminescence images were thresholded for plagioclase and the binary image was edited manually to separate touching crystals and remove artefacts. The resulting binary image was quantified using the software package

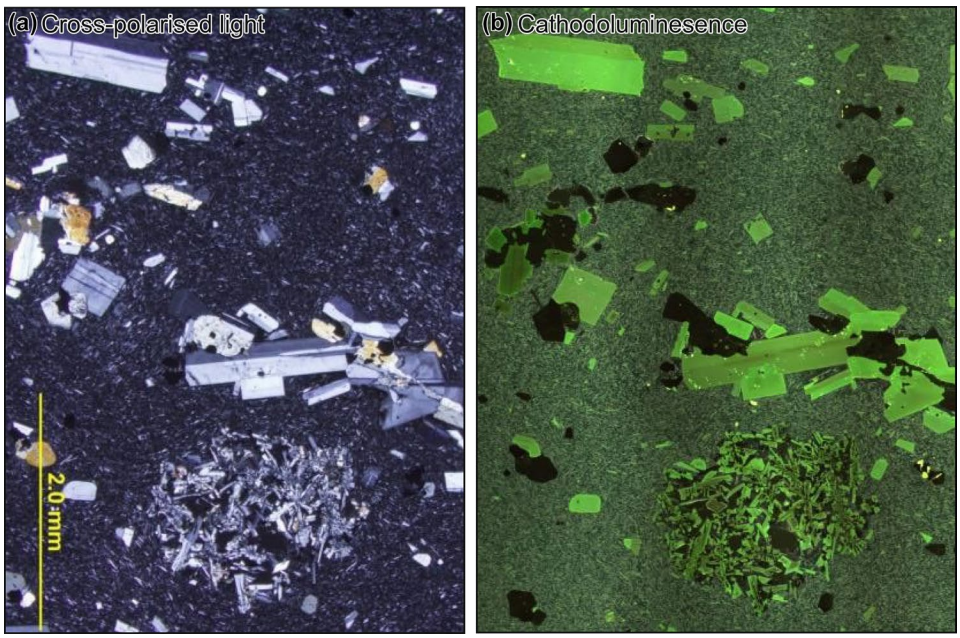


**Fig. 2** Dacite lava (NK-21) with a microgranular mafic enclave in, (**a**) linear cross-polarised image and (**b**) cathodoluminescence image. Variation in the cathodoluminescence colour of crystals is due to compositional differences and variable orientations of the crystal lattice with respect to the direction of electron illumination: hence zoning and twinning are sometimes visible. Cathodoluminescence colours: Green = plagioclase; yellow = apatite; black = pyroxenes, magnetite and vesicles. The enclave is of type A-1 according to the classification of Martin (2006)

ImageJ (Rasband 2010). The smallest crystal that could be consistently measured was 0.05 mm long.

The intersection data were converted to CSDs using the stereological program CSDCorrections version 1.6 (Higgins 2000). This method needs an estimate of the crystal shape. Overall aspect ratios were determined from the mode of intersection width/intersection length as well as the shape of [010] sections which are parallel to the tablet faces. The roundness value was determined by minimising errors in the intersection width/intersection length and total phase abundance from the sum of the intersection areas and the CSD (Higgins 2006). An overall shape of 1:3:4 and a roundness of 0.5 were used for all samples. It should be noted that plagioclase CSDs for some of our Kameni samples were originally published in Higgins (1996b) but were not converted using stereologically correct methods.

The complete CSD analyses described above were complemented by determinations of the total plagioclase content in other samples. Thin sections were illuminated using circular cross-polarised light (Higgins 2010a) and the images thresholded for plagioclase abundance.

## Our results and analytically compatible earlier analyses

### Outcrop geology

The overall characteristics of the Kameni lavas were determined in the field. All lavas are phyric with evident plagioclase crystals distributed homogeneously throughout the rock on the scale of an outcrop. Almost all outcrops of lava contain mafic enclaves, but their abundance is very variable within and between flows. In a typical outcrop of several square metres, we observed one 3 cm enclave per square meter, giving an abundance of ~ 0.07%. Parts of some flows have greater concentrations, especially the 46–47 CE flow on Palea Kameni, which has up to 5% enclaves. Most enclaves are rounded and microgranular, except in the 1950 flow in which coarse-grained plagioclase-olivine cumulates dominate.

### Petrography and CL mineralogy

The petrography of the dacite lavas is much more variable than their geochemistry (see later). The lavas have a fine-grained groundmass, with crystals of plagioclase (2.4–22%) up to 3 mm long. Clinopyroxene is much less abundant (0.1–1.7%), followed by orthopyroxene (0.3–0.7%) and magnetite (0.5–1.2%) (This study; Barton and Huijsmans 1986).The dacites contain several populations of plagioclase crystals, as is common in many intermediate volcanic rocks. Most plagioclase crystals are euhedral or subhedral with little zoning (Fig. 3a–d) and a uniform pale-green CL colour (Fig. 2b). Pale spots within the crystals in the CL images are melt inclusions, apatite crystals or artefacts due to charging (Fig. 2b). Rare plagioclase crystals have complex interior zones, with zoning and melt inclusions. These crystals mostly occur as larger, independent crystals (Fig. 3e, f). The abundance of these complex crystals is less than 2% of most lava samples. They are considered to be xenocrysts and will not be discussed further.

In the dacites, some of the plagioclase, pyroxene, and oxide crystals occur in clusters of up to about 15 crystals, commonly with an interstitial pale brown glass that is largely crystal-free (Fig. 3a, b). In the interior of the clusters the crystals are frequently small and interlocking, suggesting that initially plagioclase, pyroxene, and oxide nucleated nearby and were fused by initial crystal growth (Fig. 3c, d). Towards the exterior, the crystals have euhedral forms indicating that further growth of both phases occurred simultaneously into the silicate liquid. The larger exterior crystals strongly resemble independent crystals elsewhere in the section in shape, zoning and CL colour. The crystal clusters do not resemble the enclaves, which have a different texture (Martin et al. 2006).

Other important phases are orthopyroxene, clinopyroxene, oxides, and apatite, which also occur within the clusters as well as independent crystals. As for the plagioclase, there does not seem to be a great contrast between the forms of the independent crystals and those in the clusters. Minor apatite crystals are generally small and most are enclosed within pyroxene crystals.

The petrography of the enclaves has been described in detail in other studies and we do not want to repeat it (Martin 2005; Martin et al. 2006). All that we can add here is the plagioclase composition, as revealed by cathodoluminescence. This phase has a distinctive cathodoluminescence pattern, with a dark green interior and a pale green rim (Fig. 2) that contrasts with the pale green uniform colour of the dacite plagioclase. We do not see any crystals with similar CL colours in the dacite magma away from the enclaves.

### Overall chemical variations

The freshness and lack of alteration of samples were examined using the amount of loss-on-ignition (LOI). All subaerial samples have low LOI and are considered fresh and unaltered (appendix table 1). However, five of the samples taken underwater have high LOI (5–25%). Three samples are scoria and two are lava. If the analyses are recalculated on a volatile-free basis then the scoria samples (EN 419–91, -92, -93) do not resemble any of the volcanic rocks of the Kameni islands: they may have been modified by precipitation of calcite and dolomite in the vesicles.

Many new samples have been analysed in this study, but it behoves us to combine our data with earlier studies where

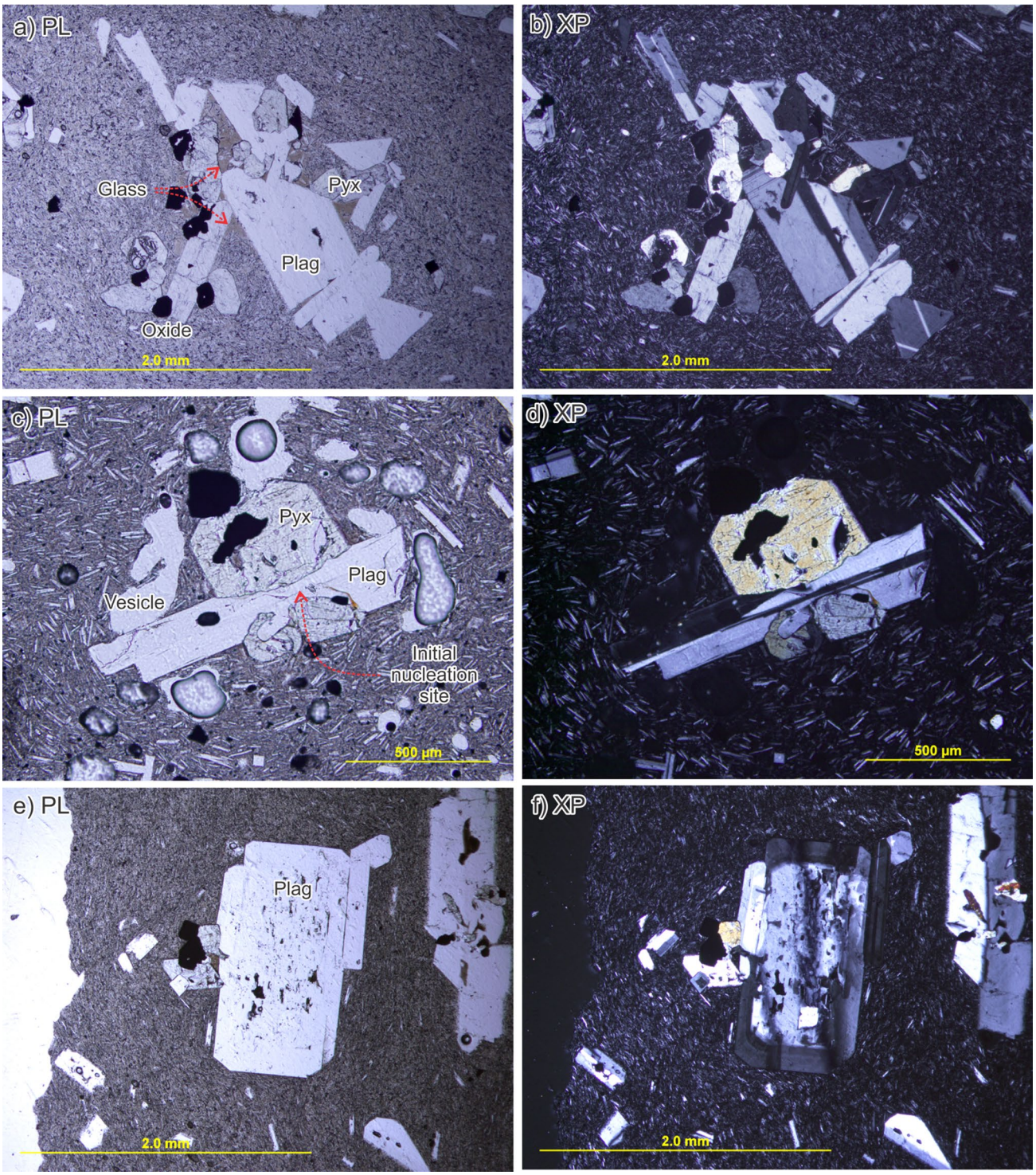


**Fig. 3** Thin sections in non-polarised (PL) and linearly cross-polarised illumination (XP). **a**, **b** Cluster of plagioclase, pyroxene and magnetite crystals. The groundmass in the interstices is glassy, with fewer microlites than away from the cluster centre. **c**, **d** Cluster of plagioclase, pyroxene and magnetite crystals. Plagioclase and pyroxene crystals are narrow near the centre of the cluster, which is presumed to be near the initial nucleation site. There are vesicles close to the crystals which are probably in contact away from the plane of the section. **e**, **f** A euhedral plagioclase crystal with a complex core and a wide, simple rim. Small pyroxene and magnetite crystals were incorporated during the growth of the rim

possible. Most major element analyses of dacites from earlier studies fall in a similarly restricted field to our analyses. However, there are significant differences, particularly in Na, which can be difficult to analyse by XRF due to the low energy of the characteristic X-rays and may also be affected by diffusion within the glass beads. There are also problems with the reproducibility of some trace element analyses, probably caused by inadequate use of standards. This is significant for the dacite analyses given the small range in compositions. For this reason, we are unable to combine early datasets and our discussion will be restricted to our data alone. In contrast, the wide range in enclave compositions, and the relatively small number analysed in this study, makes it essential to combine our data with that of other studies.

Dacite samples have been divided up into three groups: the earliest lavas from 46 to 726 CE, which are now exposed only on Palea Kameni (first phase; PK); the post-paroxysmal lavas from 1570 to 1925 CE (second phase; Nea Kameni); and the most recent eruptions from 1939 to 1950 CE (Nea Kameni). This last group is defined on the basis of its contrasting textural and chemical compositions, to be documented later.

The Total-Alkalis-Silica diagram is commonly used for the classification of volcanic rocks and their components (Le Maitre et al. 2002). All the lavas fall in a restricted group in the dacite field with silica contents from 64.0 to 68.5% (Fig. 4a, b). There is a strong correlation between silica and total alkalis. The first phase (PK) dacites have generally higher $SiO_2$ and alkali contents than the second phase dacites, but there is not a clear separation. The third phase dacites have the lowest silica contents. The enclaves have a much wider range than the lava compositions and fall in the andesite, basaltic andesite, and basalt fields. Most enclaves fall along with a relatively narrow trend with just two outliers which are from the first phase eruptions.

The affinity of the underwater lava samples can be determined using the TAS diagram. One lava sample taken close to the other NK North samples (EN 419–58) has an anhydrous composition similar to that of the other NK North samples (Fig. 4). The anhydrous composition of the other lava sample (EN 419–94) did not resemble those of the Kameni Islands. It was from a ridge SW of the Kameni islands and is hence not part of the same magmatic system. All five samples were not considered further in this study.

Magnesium contents can inform us on the role of mafic phases. MgO and $SiO_2$ are strongly correlated for the dacite lavas but with a small range in compositions (Fig. 4c). The enclaves have a much larger range in compositions, but the correlation is not so strong, especially for low $SiO_2$ samples. The division of enclave compositions into two groups for low silica contents is probably an artefact of the small numbers of analyses.

Phosphorus abundances can inform us on the role of apatite. $P_2O_5$ and $SiO_2$ are strongly correlated for the second and third phase dacites (Fig. 4d). However, the first phase dacites fall off this trend with lower $P_2O_5$ contents. These elements are also strongly correlated in most of the enclaves, except for some enclaves also from the first phase.

Zr is an incompatible element in the Kameni dacites as they do not contain zircon. There is a very strong correlation between $SiO_2$ and Zr for the dacites (Fig. 5a). Ba is also weakly correlated with Zr (Fig. 5b). In both diagrams, there is an overall trend to lower $SiO_2$, Zr, and Ba with the progression of the eruptions.

Incompatible element ratios are unchanged by fractional crystallisation of major minerals and can be used for examining compositional variations in the source materials (Fig. 5c). The dacites show a slight difference in Th/Ta between samples from the three phases. However, the enclaves show a considerable variation in both Th/Ta and Zr/Nb (Fig. 5c).

Rare-earth elements (REE) are very useful for understanding the role of plagioclase in magmatic systems due to the anomalous behaviour of europium with respect to its neighbouring REE. The easiest way to express REE variations is in terms of Eu/Eu* (Eu anomaly) versus $La_N/Lu_N$, which reflects the overall slope of the chondrite normalised REE spectrum (Fig. 5d). All of the dacite samples have a small range in Eu/Eu* values (0.67–0.78) which are negatively correlated with $La_N/Lu_N$. There is a general trend to smaller Eu anomalies and shallower REE patterns with the progression of the eruptions. Enclaves have a much wider range of values with a negative correlation between Eu/Eu* and $La_N/Lu_N$. Almost all enclaves have Eu deficits (Eu/Eu* < 1).

## Secular chemical variations

Secular variation in the overall composition of dacite lavas can be determined because the age of most flows is well known. The only exception analysed here is the NK North flow: its age is between 1848 and 1925 but has been arbitrarily placed at 1900 CE in Fig. 6a. The compositional variation shown by dacites and enclaves in our new data mirrors that of earlier studies (Huijsmans 1985; Martin 2005; Zellmer et al. 2000) and hence the datasets can be considered together. $SiO_2$ has been chosen as a key parameter for characterising the magmas in each flow group, as the uncertainty in its determination is much less than the variation in the data. The simplest way of illustrating this data is with a linear graph of time versus composition (Fig. 6a). The overall trend is clear: medium $SiO_2$ contents in the earliest flows rise in the 726 flows and then descends slightly with much higher dispersion in the 1570–1950 eruptions. Although this graph preserves a linear time

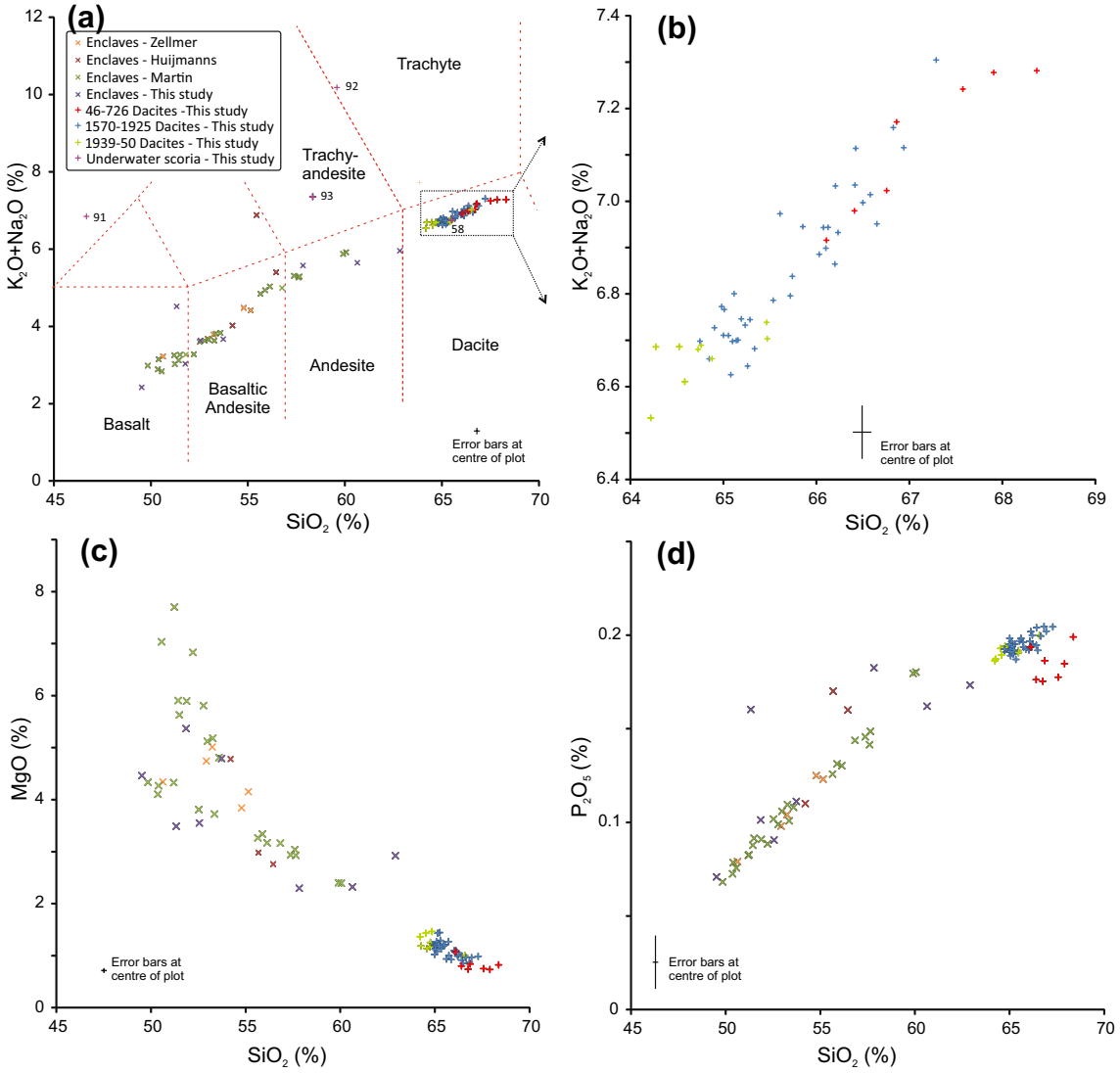


**Fig. 4** Major element compositional data for dacites (this study) and micrographic enclaves (this study; Huijsmans 1985; Martin 2005; Zellmer et al. 2000). Analyses of the underwater scoria samples have been recalculated on a volatile-free basis. **a** Total-alkalis-silica diagram (Le Maitre et al. 2002). Underwater sample numbers are abbreviated: 91 = EN 419–91. They fall away from the main trend and are hence assumed to have been severely altered. They will not be considered in further discussions. **b** Detail of TAS diagram for dacites analysed in this study. **c** MgO versus $SiO_2$. **d** $P_2O_5$ versus $SiO_2$

component, variations in recent data are not very clearly shown. Hence, we have plotted $SiO_2$ content for each eruption (Fig. 6b). The overall pattern is similar for the older flows, but this figure reveals better the variations in the younger eruptions. Eruptions from 1570 to 1940 have a similar, relatively wide range in $SiO_2$ composition. However, lower $SiO_2$ samples become more common with time and dominate the 1950 eruption.

Enclave $SiO_2$ contents have a wide range in values but show groupings for certain eruptions, although we must acknowledge the relatively small number of enclaves analysed from older events (Fig. 6c).

## Plagioclase abundance variations

Plagioclase abundance in dacites was determined from the sum of the area of crystal outlines and varies from 2.4 to 22%. The earliest flows have about 4–7% plagioclase crystals, which descends to its lowest value in the 726 CE eruption products (Fig. 7a). After that event, plagioclase abundance generally increases, reaching the highest values in the 1950 eruption. The plagioclase content is also related to the $SiO_2$ content of the magmas: most low $SiO_2$ magmas have medium to high plagioclase contents, whereas more silicic magmas tend to have lower plagioclase contents (Fig. 7b).

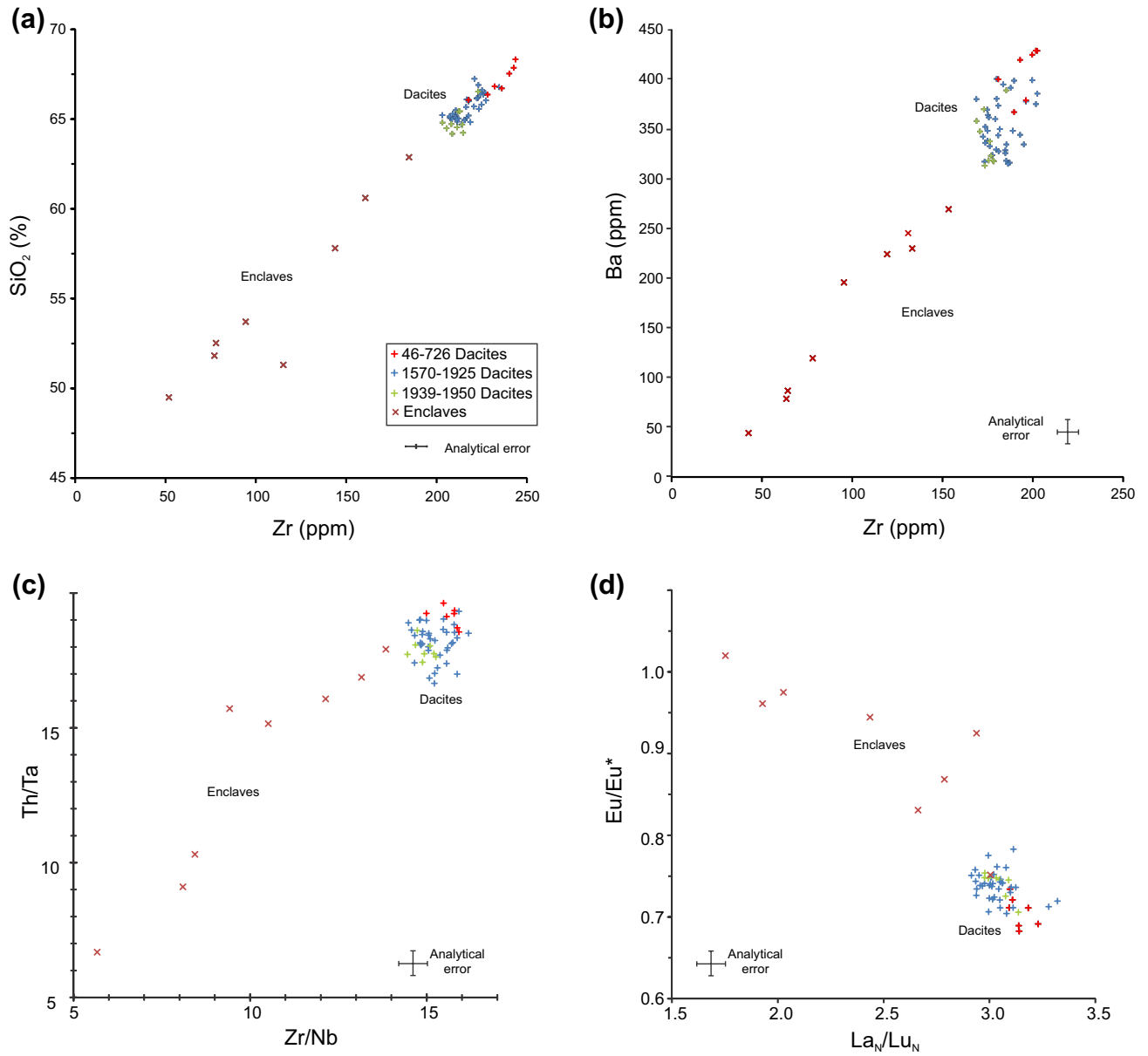


**Fig. 5** Trace element variations in enclave and dacite data from this study. **a** $SiO_2$ versus Zr. **b** Ba versus Zr. **c** Incompatible element ratios. **d** Europium anomalies versus REE normalised slope. Analytical error estimates do not account for error correlations and are hence probably overestimates in panels **c** and **d**

There is very little variation in $Al_2O_3$ content with plagioclase abundance, but the analytical error is large as compared to the overall variation (Fig. 7c). Although there is much dispersion, plagioclase content is broadly correlated with Eu/Eu* values, with a general increase with eruption date (Fig. 7d).

### CSD variations

All dacite CSDs are strongly curved, concave up (Fig. 8a, electronic appendix 1). The lower size limit is controlled by the smallest crystal outline that could be measured (0.04 mm) and the accumulation of correction errors in for the smallest size bins (Higgins 2000). Hence, the CSD is undefined below 0.1 mm.

There is strong theoretical and experimental evidence that CSDs in many simple systems are straight on a semi-logarithmic diagram (Cashman and Marsh 1988; Marsh 1988). Curved CSDs can be produced in many situations (Higgins 2006), but the most popular involve mixing of two crystals populations (Higgins 1996b) or crystallisation under two different cooling regimes (e.g. Fornaciai et al. 2015). Such

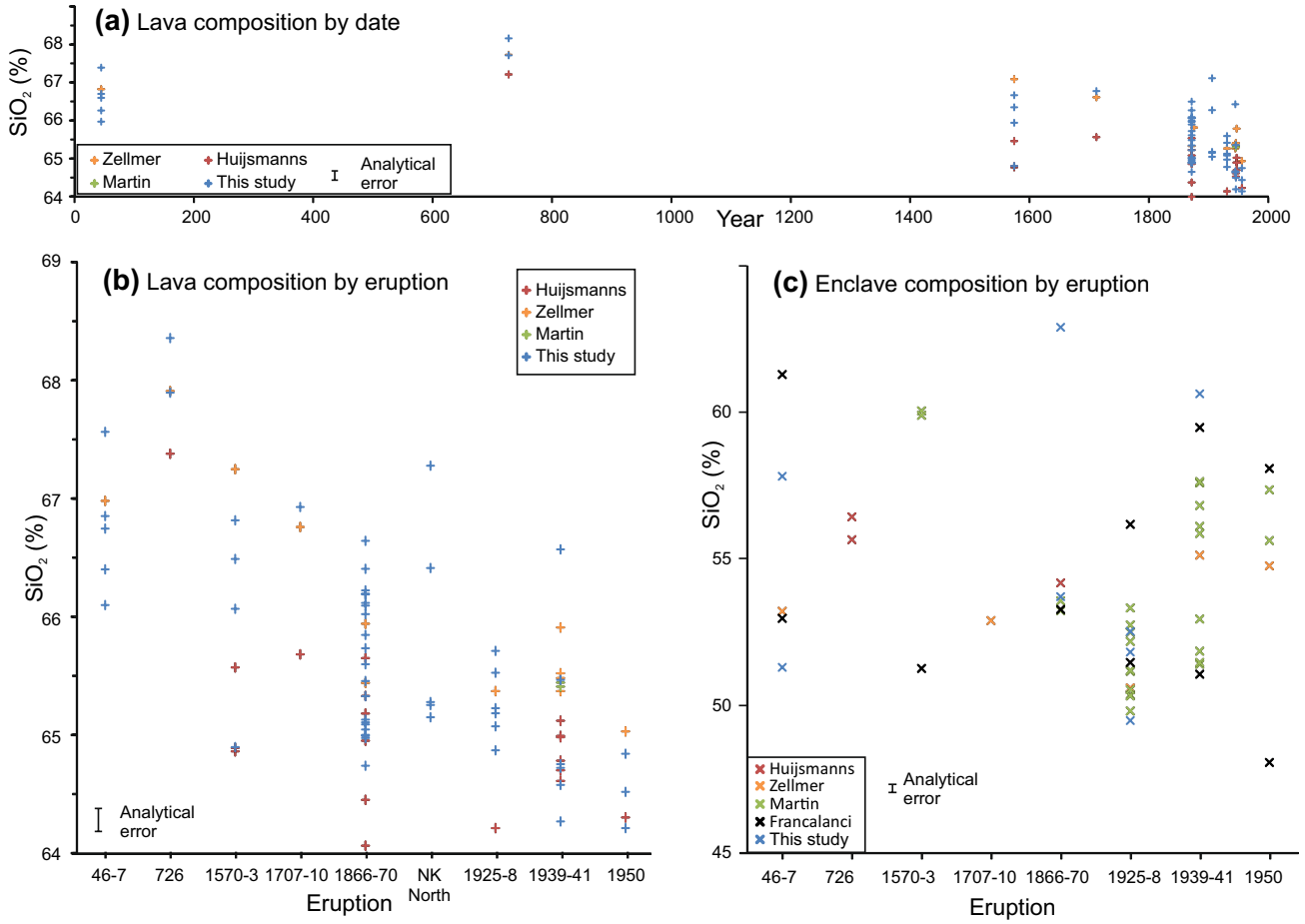


**Fig. 6** **a** Variation of dacite $SiO_2$ contents with eruption date. **b** Variation of dacite $SiO_2$ contents for different eruptions. **c** Variation of enclave $SiO_2$ contents for all the eruptions (no data from NK North; this study; Huijsmans 1985; Martin 2005; Zellmer et al. 2000)

curved CSDs can be modelled by summing two straight CSDs (Fig. 8B) and fitting the curve by trial and error to the measured CSD (Higgins 1996a). One population has a steep slope with many small crystals and is termed microcryst, whereas the other population has a shallow slope and abundant large crystals and is termed macrocryst.

The slope of a CSD has units of 1/length, hence it is easier to characterise the distribution using the characteristic length (CL) which equals − 1/slope of the fitted line and has the units of length. For a straight CSD, it is equal to the mean crystal size. The curvature of the CSD can then be easily expressed on a graph of plagioclase abundance versus characteristic lengths of the two components. It is then much easier to compare curved CSDs from different samples using this approach than simply to plot all the CSDs together on the same diagram (Fig. 9).

The range of CL values of the microcryst population is almost constant for all samples except those from the last two eruptions (Fig. 9a). Similarly, the range in CL of the macrocryst population is great for all samples except those from the last two eruptions (Fig. 9a).

It is of interest to determine the relationship between the CLs of the two model crystal populations and the repose time between eruptions (Fig. 9b). This has been calculated for the subaerial eruptions only, as we do not know the exact age of all underwater eruptions. For the 46–7 CE eruption, the predecessor is assumed to be the 197 BCE eruption, whose products are no longer visible, but there may have been other eruptions that never reached the surface, in which case the repose time would be shorter.

The microcryst populations have small CLs for the short repose times of the latest eruptions (1939–41, 1950), and the range of CLs is greater for longer repose times of the first and second eruptive phases. The macrocryst populations have rather similar CLs for all repose times. However, the four samples with greater CLs all have repose times greater than 150 yrs.

The abundance of plagioclase in the two model populations can be compared with their chemical composition, as was done in Fig. 7 for the total crystal population. There is an overall negative correlation between silica content and macrocryst plagioclase abundance (Fig. 9c)

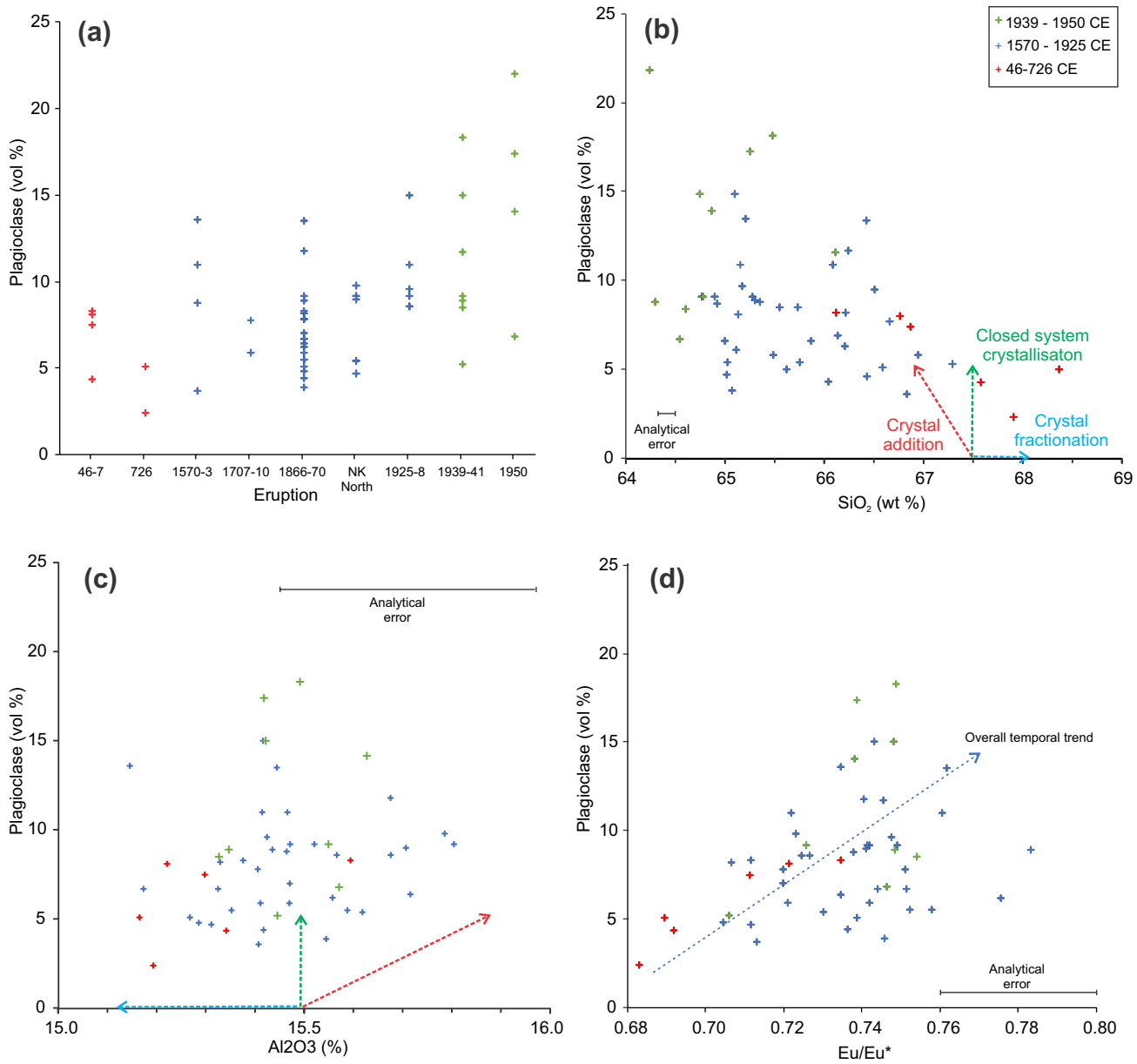


**Fig. 7** Plagioclase total volumetric abundances were determined from textural data and have errors smaller than the symbol. **a** Plagioclase abundance for different eruptions. **b**, **c** Plagioclase abundance versus $SiO_2$ and $Al_2O_3$ content. Vectors show variations for addition, crystallisation or fractionation of 5% plagioclase $An_{50}$. **d** Plagioclase abundance versus Eu/Eu*

as well as a secular variation in both these parameters. This correlation is not significant for the microcryst population abundances (Fig. 9d). Similarly, there is no significant correlation between alumina and macrocryst abundance (Fig. 9e). However, there is a correlation between europium anomaly and macrocryst abundance (Fig. 9f).

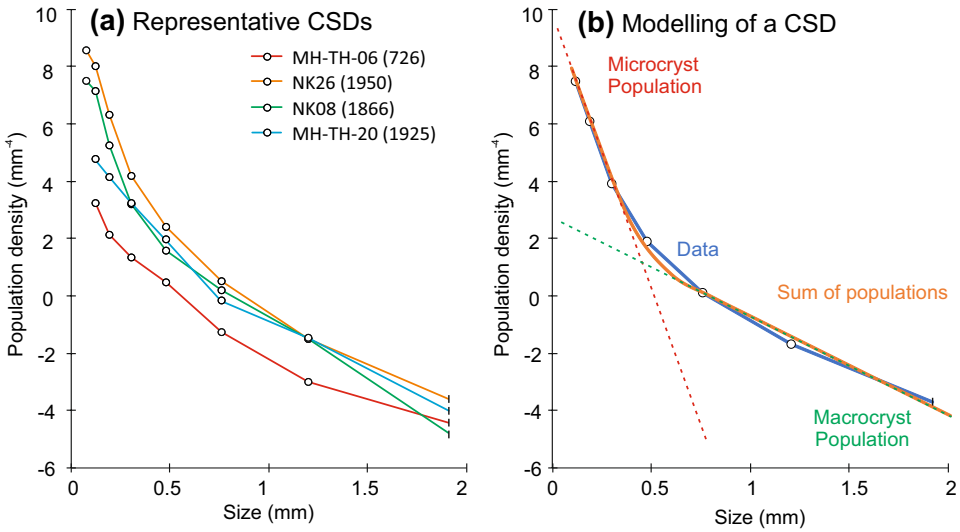


**Fig. 8** **a** Representative plagioclase CSDs from the Kameni dacites. Complete CSD data is in electronic appendix 1. **b** Kameni CSDs have been modelled by the addition of two straight CSDs (here for sample NK25), a population of smaller crystals termed microcrysts and a population of larger crystals termed macrocrysts, following Higgins (1996a)

## Discussion

### Existing models for the Kameni system

Many of the existing studies of the Kameni volcanic rocks have tried to constrain the properties of the magmatic plumbing system that fed the Kameni eruptions. The earliest models envisaged that plagioclase and other phases crystallised throughout the magma reservoir and descended by gravity towards the lower part of the reservoir, creating a stratified reservoir (Fig. 10) (Barton and Huijsmans 1986). Eruptions during the last 2000 years sampled successively lower levels of this reservoir, with increasing plagioclase contents. Such a model requires that the temperature remain constant and hence that the magma reservoir must have been large, or more likely, that it was frequently reheated by the influx of new mafic magma. However, the main weakness of this model is that such additions of heat would necessarily produce convection, which would destroy the stratification. In addition, the high viscosity of the dacite magma would inhibit the gravitational transfer of crystals.

Other models have been proposed in subsequent studies. Higgins (1996b) proposed that there were two magma reservoirs. Eruptions were rooted in the upper one which was topped up from a deeper reservoir before each event. Francalanci et al. (1998) and Petrone et al. (2013) proposed that magmatic diversity of the dacite and the enclaves were produced by mingling and mixing between the dacite and mafic magmas that are injected into the dacite. The work of Martin et al. (2006) was mostly concerned with the origin of the enclaves and not of the dacites themselves. All these models were based on the study of either chemistry or texture: in this study, we use these complementary datasets to modify existing models and propose a new mechanism for the production of magmatic diversity in the Kameni volcanic system.

### Origins of magmatic diversity

#### Enclaves

Enclaves are a very minor, but widespread component of the Kameni lavas and it is important to determine their role, if any, in the development of magmatic diversity. The broad collinearity between the dispersion of dacite compositions and those of the enclaves has suggested to some authors that magmatic diversity was produced by mixing between primordial dacite and mafic magmas (Francalanci et al. 1998). Such a model would be expected to produce a continuous spectrum of compositions, from the most mafic enclave to the most silicic dacite. We have combined data from all available sources and show in Fig. 4 that this is clearly not the case and there is a conspicuous gap between the dacite and enclave compositions. The enclave compositions do not lie on a linear trend, hence at least three end-member components are necessary for an origin by mixing.

Petrone et al. (2013) suggested that there was a field and petrographic evidence for disaggregation ('crumbling') of enclaves in the Kameni lavas. Our cathodoluminescence images are a sensitive test for such a process. As we mentioned before, plagioclase crystals in enclaves are generally small and have a distinctive cathodoluminescence pattern, with a dark green interior and a pale green rim (Fig. 2). There are no crystals with this pattern in the dacite. Indeed, there is a distinct paucity of crystals of this size in the dacite. Hence, if the enclaves have been disaggregated, then the crystals must have been completely resorbed. Enclaves from different eruptions have, in some cases, distinctive compositions that contrast with that of earlier or later eruptions

(Fig. 6c). This suggests that enclaves have a relatively short life in the magma reservoir as is suggested by experimental studies (Ruprecht et al. 2020). All these arguments indicate that although enclaves are an important indicator of mafic input to the base of the magma reservoir, they have not influenced the composition of the dacites in a significant way.

Even if the enclaves did not modify significantly the composition of the dacites, the mafic magma that produced them may have had another important role in the magmatic development of the system. Most of the enclaves are vesicular, showing that vapour saturation was achieved by cooling after the mixing event. At this time the crystal network was sufficiently strong that the enclave could not expand, so most of the exsolved gas must have escaped into the surrounding magma, where some bubbles may have become attached crystals in the mush (Pleše et al. 2018). This idea will be developed later.

### Crystal clusters in the dacites

The degree of clustering of crystals in volcanic rocks is very variable, but its petrological significance has rarely been explored. In the Kameni dacites, many crystals of plagioclase, pyroxene, and magnetite are clustered and there does not appear to be any clear mineralogical differences between clustered and independent crystals (Fig. 3a, b). Crystals within the cores of the larger clusters are generally smaller than crystals in the exterior of the cluster and independent crystals. In some cases, narrow crystals in the core widen out in their more peripheral parts (Fig. 3c, d). This suggests that the crystals initially nucleated and grew near to each other, in an environment where all major phases could nucleate and grow. The simplest explanation is that crystallisation occurred in a peripheral region, perhaps at the base of a magma reservoir, where the density of the clusters would reduce the likelihood of dispersion by simple magma convection. However, it is clear that clusters have been disrupted and dispersed, indicating the need for special events, such as the input of new mafic magma into a semi-consolidated crystal mass.

The preservation of glass between the crystals in the interior of the clusters suggests that the clusters have been cooled more rapidly than the surrounding magma. One possible mechanism is by attachment of bubbles from the enclaves to crystals in the basal part of the reservoir. The resultant buoyance of some crystal–bubble couples would have disrupted the mush and enabled rapid uplift of crystal clusters. We will return to this model below.

### Nature of the crystal cargo

We can now discuss the origin of the remarkable variability in the abundance of crystals in the dacites and if it can inform us about magmatic processes active in the Kameni volcanic system. Crystals in lavas can be phenocrysts, which grew in place from their surrounding magma, antecrysts, which grew in a distant, but the magmatically connected environment, or xenocrysts, which come from a separate system. Isolated xenocrysts can be recognised by their complex zoning (Fig. 3e, f), but they are not abundant and will not be considered further. Sub-volcanic magmatic systems are generally complex, with transfer and mixing between different magmatic reservoirs in each of which crystallisation can occur and here the problem is to choose the simplest system that can account for the observed chemical and textural variations.

We will first consider the possibility that the whole crystal cargo (microcrysts and macrocrysts) is dominantly antecrysts, incorporated in the magma by mixing of a crystal-rich material with a sparsely-phyric magma. The most abundant phase in the dacites is plagioclase, hence here we model the effects for plagioclase of composition $An_{50}$—the inclusion of other phases seen in the clusters does not make a significant difference to the modelling (Barton and Huijsmans 1986). The addition of plagioclase to a single magma produces a simple diagonal variation in a plot of plagioclase abundance versus $SiO_2$ (Fig. 7b). Our data show a band of variations, which necessitates multiple original magma compositions. Most of the dispersion can be accounted for by the addition of 4–20% plagioclase to magmas with original $SiO_2$ contents of 66–68%. However, such a model is unable to explain the variation in $Al_2O_3$ with plagioclase abundance (Fig. 7c), hence the simple, pure antecryst model is rejected. We will discuss later the possibility that only the larger crystals (macrocrysts) were added.

Growth of plagioclase phenocrysts in the Kameni dacites is very probable, but the high viscosity of the dacite magma and the small contrast in density makes it unlikely that significant gravity-driven fractionation could occur by compaction or settling. Involvement of other, denser phases, as suggested by the occurrence of polymineralic clusters in the dacite lavas, would give a greater density, but probably not enough to make a significant difference. In this case, the overall composition of the magma would be unchanged by crystallisation. This model would produce a vertical dispersion on the plot of plagioclase abundance versus chemical composition (Fig. 7b–d). However, there are significant chemical variations and hence this simple model must be rejected. One possible modification would be crystallisation from multiple original magma compositions. In this model, the earliest lavas would have formed from the most evolved magmas (highest $SiO_2$ and lowest $Al_2O_3$) and have shown the least amount of crystallisation. Later lavas would have formed from progressively less evolved magmas and crystallised more, culminating in the high-crystallinity 1939–1950 magmas. The observed Eu/Eu* values (Eu anomaly) are

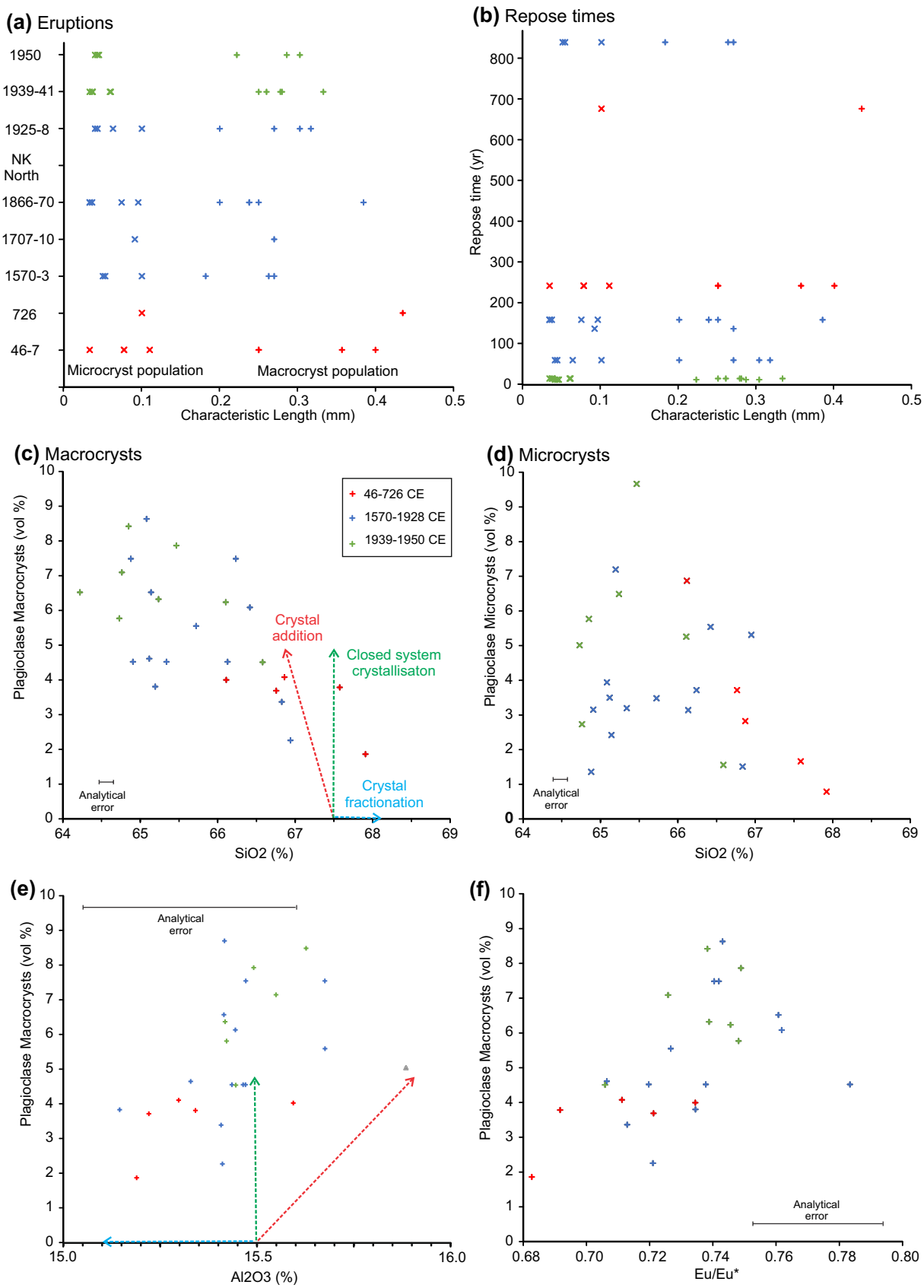
(a) Eruptions
1950
1939-41
1925-8
NK North
1866-70
1707-10
1570-3
726
46-7
Microcryst population
Macrocryst population
Characteristic Length (mm)
(b) Repose times
Repose time (yr)
Characteristic Length (mm)
(c) Macrocrysts
46-726 CE
1570-1928 CE
1939-1950 CE
Crystal addition
Closed system crystallisaton
Crystal fractionation
Analytical error
Plagioclase Macrocrysts (vol %)
SiO2 (%)
(d) Microcrysts
Plagioclase Microcrysts (vol %)
SiO2 (%)
(e)
Analytical error
Plagioclase Macrocrysts (vol %)
Al2O3 (%)
(f)
Analytical error
Plagioclase Macrocrysts (vol %)
Eu/Eu*

◂**Fig. 9** **a** CLs of microcryst and macrocryst model plagioclase populations versus eruption. **b** CLs of the two populations versus repose time. **c** Silica versus macrocryst model abundance. The vectors are for plagioclase of composition $An_{50}$. **d** Silica versus microcryst model abundance. **e** Alumina versus macrocryst model abundance **f** Europium anomaly versus macrocryst model abundance

consistent with such a model: the earliest, most fractionated magmas have the smallest values (Fig. 7d). Hence, a model is preferred in which the crystal cargo is essentially dominated by phenocrysts that grew within the main magma reservoir. However, we cannot rule out the possibility that some crystals are antecrysts that were added from connected reservoirs.

### Textural constraints on magmatic processes

The curved plagioclase CSDs observed in the Kameni dacites were first interpreted as evidence of mixing of two different magmas (Higgins 1996b). However, the uniformity of the plagioclase macrocryst populations and the lack of chemical evidence for simple mixing weakens this model. Hence, we favour here an origin for the curved CSDs by crystallisation under two different pressure and temperature regimes, represented by the characteristics of the two straight CSDs used in the modelling.

The microcryst population is dominated by the smallest crystals and represents a growth event immediately before the eruption. The steep slope indicates that growth occurred at significant undercooling, presumably in a shallow magmatic reservoir. The characteristic length of this population tends to be smaller for the latest eruptions (Fig. 9a). There does not appear to be a correlation between characteristic length and repose time (Fig. 9b).

The macrocryst population reflects an earlier phase of plagioclase growth. Most samples have similar characteristic lengths for different flows (Fig. 9a), except for four samples with much greater characteristic lengths. These all have lower plagioclase contents and most erupted during the PK phase. Characteristic length is broadly correlated with repose time, except for two samples from the 1570 CE flow which have the longest repose times (Fig. 9b).

CSDs with greater characteristic lengths can be produced by textural coarsening, in which small crystals dissolve and large crystals grow (Higgins 2010b). Coarsening develops when a magma is maintained for some time close to the mineral saturation temperature and may be accelerated if the temperature oscillates around this value (e.g. Mills and Glazner 2013). The infrequency of eruptions during the PK phase may have led to a stable environment that permitted coarsening. The lack of small, recently nucleated, crystals in the glassy parts of the clusters (Fig. 3a, b) suggests that the clusters must have coarsened, presumably at the base of a deep magma reservoir. These crystal-free glasses were then preserved by rapid uplift.

Characteristic crystal growth times can be determined if the growth rate of plagioclase can be established (Marsh 1988). Cashman (1993) established a correlation between growth rate and cooling time for plagioclase in mafic magmas and a similar relationship is generally assumed for more felsic magmas. For the microcryst population a cooling time of 3 years, which accords with seismic data from the 2011–12 magma injection event, would suggest a growth rate of about $10^{-9}$ mm/s. Such a value would indicate characteristic growth times of 1.4–3.5 years for the microcryst population. The shortest times are associated with the 1939–41 and 1950 flows, which have the shortest repose times and highest plagioclase contents. The macrocryst population may have formed in a deeper reservoir and hence the growth rate may have been lower: Higgins (1996b) used a growth rate of $10^{-10}$ mm/s, which would give characteristic crystal growth times of 60–160 years. This broadly accords with repose times of 150–250 years for three of the four coarsened populations (Fig. 9b).

Pertinent temporal constraints on magmatic processes in the Kameni systems have been determined using other methods. Ra/Th ratios in Kameni rocks suggest that crystallisation of plagioclase occurred less than about 1000 years before eruption (Zellmer et al. 2000). Trace element profiles in plagioclase suggest a residence time of 100–450 years (Zellmer et al. 1999). In contrast, Martin et al. (2008) used trace element profiles in an olivine crystal from a cumulate enclave in the 1925–8 lavas to conclude that mafic magma was added only a few months before the eruption. These data will be used to constraint a magmatic model.

The total macrocryst population can be compared to various chemical parameters as was done earlier for the whole crystal population (Figs. 7, 9). As before, it is not possible to generate the observed dispersion only by the addition of plagioclase to a single liquid composition. However, here the model fits better on the graph of $Al_2O_3$ versus macrocryst abundance (Fig. 9e) than on the graph of $SiO_2$ versus macrocryst abundance (Fig. 9c). Again, the data support a model of closed-system crystallisation from liquids of variable composition.

### Magmatic development by bubble-mediated liquid and crystal movements

The chemical and textural data presented above suggest that Kameni magmas were formed by the closed-system crystallisation of variable amounts of plagioclase, and lesser amounts of other phases, from a range of dacite liquids, but how was this achieved? The presence of crystal clusters shows that much of the plagioclase macrocrysts formed in an environment with a high crystal content. The density of

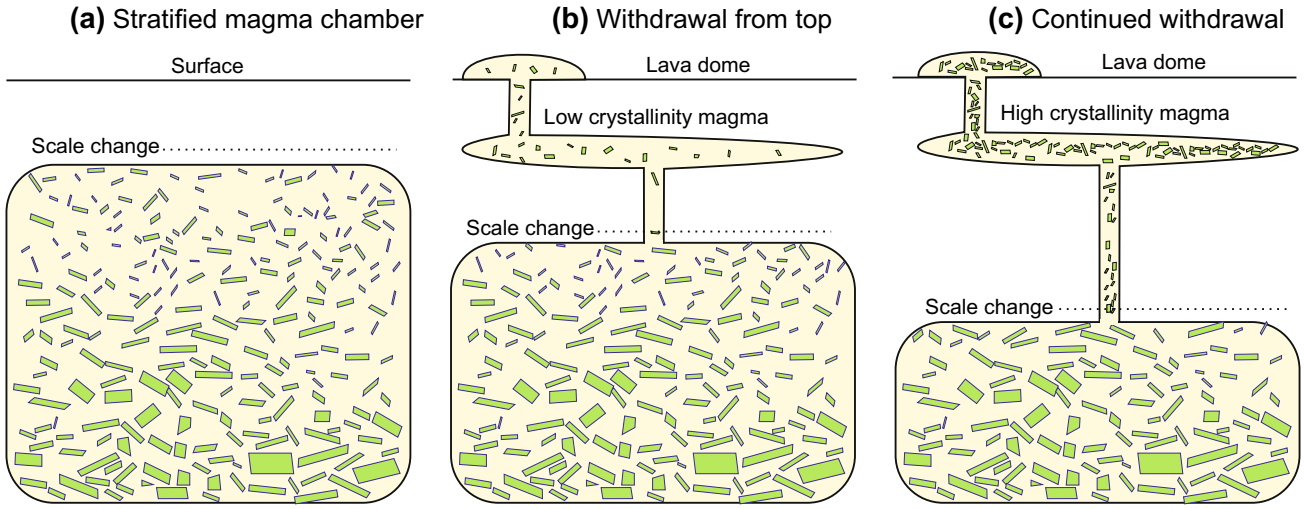


**Fig. 10** Schematic model of a static, stratified magma reservoir following the work of Barton and Huijsmans (1986). **a** A stratified magma reservoir is created by crystallisation of plagioclase and other phases followed by accumulation in the lower part of the reservoir. **b** The first magma to be withdrawn is from the upper, low crystallinity part of the reservoir. **c** The magma reservoir is emptied and successively higher crystallinity magmas are withdrawn

plagioclase is close to that of the magma, hence this zone cannot have formed by gravity-driven accumulation: instead crystallisation must have occurred in situ, probably largely at the base of the reservoir. The degree of connectedness of the individual crystals was probably very variable. This high-crystallinity material was subsequently disaggregated into clusters and individual crystals and incorporated into the dacite liquid. Simple recharge of the reservoir with mafic magma cannot lift enclaves, otherwise we would see abundant enclaves in all dacites, which is not the case. Hence, it is proposed that the buoyant forces necessary to disrupt the basal crystal mass and lift the material to the top of the reservoir were produced by the physical association of crystals with vapour bubbles. Such a process has been proposed for the origin of crystal-bearing vesicle pipes (e.g. Helz 1987), but not for crystals and crystal clusters in a magma reservoir.

Interactions between bubbles and crystals at the base of a magma reservoir have been explored in several recent papers. Mungall (2015) modelled mathematically the problem of non-wetting bubble migration through a basal accumulation of crystals and concluded that bubbles would be trapped in a cumulate. Boudreau (2016) used an analogue experiment to show exactly the opposite—that non-wetting bubbles can escape from cumulates easily. However, both studies may not be completely applicable to natural systems as Pleše et al. (2019; 2018) showed that bubbles nucleate and grow on plagioclase and pyroxene crystals and hence that these surfaces are wetted. If the bubble–crystal couples stay together long enough then they will rise buoyantly in the reservoir through the dacite magma. There, there may be sufficient time for the bubbles to detach, which is why we do not see many bubbles on the crystals now (Pleše et al. 2019; 2018). This model can be used to construct a model for magmatic development in the Kameni system.

We propose that magmatic development started in a deep dynamic magma reservoir, or a nexus of magma storage areas filled with low-crystallinity dacite magma, where two different scenarios may have developed, here termed juvenile and mature (Fig. 11). Paradoxically, the juvenile scenario appears to be applicable to the later magmas, and the mature model to the earliest magmas.

The juvenile model is invoked for low to high crystallinity, less chemically evolved magmas mostly produced after the 726 CE paroxysmal event. Crystallisation occurred at the base of the reservoir, producing a loose mass of crystals that were cemented in places by further growth (Fig. 11a). Mafic magma was injected into the base of the reservoir where it was cooled by the dacite and became saturated with vapour. Vapour pockets developed in the semi-crystalline enclaves and grew until bubbles were forced out of the enclaves into the dacite magma. Here, some of the bubbles attached to silicate crystals. Buoyance of the crystal–bubble couples disrupted the crystal mush. The couples then rose rapidly and accumulated at the top of the reservoir, where the interstitial liquid in the crystal clusters solidified as glass. Thermal convective movements induced by the mafic input may have contributed to the uplift process. Subsequent eruptions may have sampled both the high crystallinity magmas at the top of the reservoir or the lower crystallinity magma beneath this layer.

In the mature model, crystals of plagioclase, pyroxene and oxides, nucleated and grew at the base of the reservoir until the crystals impinge on each other forming a rigid network (Fig. 11b). This crystal network may have formed

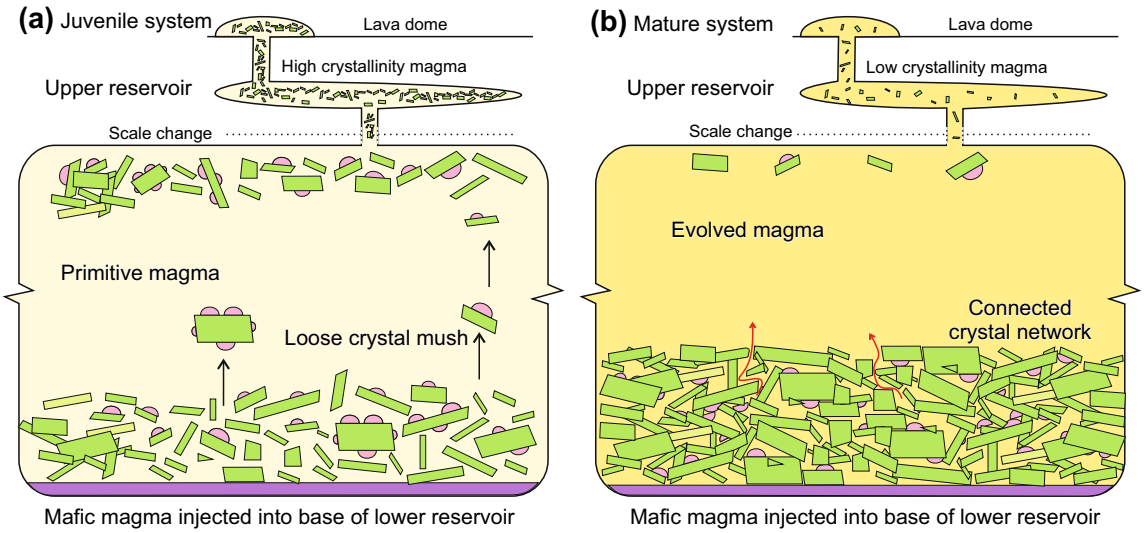


**Fig. 11** Schematic dynamic magma reservoir models for producing magmas of variable chemical composition and crystallinity. The lower and upper components are not all at the same scale and are shown for a single, simplified magma storage and transfer system. In both the juvenile (**a**) and mature models (**b**) the process starts with the creation of a reservoir filled with dacite magma. Cooling and crystallisation produce a crystal mush at the base of the reservoir. This mush is initially made of loose crystals (**a**) but with time growth will fill in interstitial space to make a semi-rigid connected network (**b**). In both models mafic magma is injected into the base of the reservoir, causing vesiculation. In the juvenile system (**a**), the loose mush is disrupted by bubbles out-gassed from the mafic magma. Some bubbles will adhere to the crystals in the dacite and make crystal-bubble couples that rise in the magma reservoir. Bubbles may detach when the couples are stored on the roof. Accumulation of crystals near the roof will produce a high-crystallinity magma that is relatively primitive as the original liquid composition is almost unchanged. For the mature system (**b**), the crystal network acts as a rigid filter and the bubbles will force out evolved magma that was originally between the crystals into the magma reservoir. Minor parts of the mush may be mobilised in the same way as in the juvenile system and rise to the top of the reservoir, forming a chemically evolved low-crystallinity magma. In both juvenile and mature systems, the magma in the upper part of the reservoir does not necessarily erupt directly but instead may feed an upper chamber from where it may be stored or erupted

because the host rocks were relatively cool at the start of the eruptive cycle, allowing for more growth. However, CSDs suggest that some crystal-bearing regions were coarsened, which would have maintained channels for the subsequent escape of interstitial magma (Higgins 2006, p. 67). The interstitial silicate liquid was isolated and evolved towards more silicic compositions by fractional crystallisation. As in the juvenile system, injection of mafic magma into the base of the reservoir produced enclaves with vapour pockets. Again, bubbles were transferred to the dacite crystal network where they attached to the silicate phases. However, buoyant forces could not overcome the strength of the network, so the vapour pocket instead displaced the interstitial fractionated liquid which mixed with the dacite liquid in the reservoir. This evolved liquid may have picked up some loose crystals from the top of the pile that rose to the top of the reservoir to produce a low-crystallinity, chemically evolved magma.

The presence of gabbroic cumulate enclaves in the 1950 CE flow suggests that bubble-mediated crystal floatation may have removed all crystals that formed from the dacite magma and excavated down to the underlying mafic unit. Here, slow cooling would have coarsened plagioclase and olivine that originally crystallised from the mafic magma. Bubbles could have wafted these materials into the magma forming what we see now as gabbroic enclaves.

In both these models, magma may have been withdrawn from the top of the lower reservoir directly or transferred to a sub-volcanic reservoir. The latter seems to have been the case for the 2011–2012 CE intrusive event (Newman et al. 2012; Parks et al. 2012). The trigger for such a transfer may have been mafic magma injection in the lower reservoir (Rizzo et al. 2015).

Chemical and textural data can be used to constrain the timing of the magmatic models. The macrocryst population characteristic growth times, Ra/Th ratios (Zellmer et al. 2000) and plagioclase trace element profiles (Zellmer et al. 1999) all suggest that plagioclase grew in the lower magma reservoir in less than 1000 years (Fig. 11). The microcryst population characteristic growth times suggest storage in the sub-volcanic upper reservoir for up to a few years, which fits with seismic evidence from the 2011–12 CE event (Newman et al. 2012). The olivine trace element profile indicates a short transition time for an enclave between the base of the lower reservoir and the surface (Martin et al. 2008). Perhaps this reflects different movements of enclaves and plagioclase macrocrysts in the lower reservoir. It may also confirm that

storage times in the upper reservoir are short-less than a few months.

## Conclusions

The Kameni volcanic centre has produced dacitic magmas that show a limited range in chemical composition, but a huge range in textures, clearly expressed in the abundance of plagioclase crystals. We propose that the observed chemical and textural diversity was produced by interactions between basal crystal masses and bubbles. Two extreme situations can be identified: Juvenile and mature systems.

In a juvenile system, the crystallisation of plagioclase and other phases at the base of a lower magma reservoir creates a loose network of crystals. In some areas, growth will link crystals to form small connected clumps. Injection of mafic magma into the base of the reservoir produces enclaves that are saturated in vapour. Expansion of the gas pockets in the enclaves will lead to the escape of bubbles into the dacite and their attachment to silicate crystals. Buoyant forces then disrupt the loose crystal mass and bubble–crystal couples rise towards the top of the reservoir where they accumulate to be tapped periodically to feed eruptions. This process produces a less chemically evolved magma, with a crystal content that can range to high values.

In the mature system, more protracted crystallisation of plagioclase and other phases at the base of a magma reservoir creates a strongly-connected network of crystals. Again, vapour pockets are produced in enclaves of mafic magma and bubbles escape to adhere to the silicate phases in the crystal network of the reservoir. However, in this model, the bubbles displace the evolved interstitial liquid which mixes into the body of the magma reservoir. The ejected magma may also pick up a small number of bubble–crystal couples from the top of the mush zone which rise in the reservoir. This process produces a crystal-poor but chemically evolved magma at the top of the reservoir.

In both situations, there may have been periodic withdrawal of magma from the top of the reservoir to a high-level staging volume, from which the magma may have erupted periodically to produce the diverse magmatic compositions observed in the Kameni lavas.

The juvenile system was more important for the more recent eruptions, whereas the mature system seems to have dominated the oldest eruptions. This may reflect the generally decreasing repose times of the system, which allowed for the development of an interconnected mush zone at the base of the magma reservoir.

**Acknowledgements** We would like to thank Steve Carey for supplying the underwater samples. Pantelia Sorotou gave us tremendous help on the islands. We would like to thank the Santorini Union of Boatman for their help with access to the islands, particularly Mr Thanasis who landed us in difficult spots. Comments of anonymous reviewers considerably improved the manuscript.

**Funding** MDH-Natural Sciences and Engineering Research Council (Canada); JVA-Fonds de la Recherche Scientifique (Belgium).

**Data availability** Data will be provided in a data repository.

### Compliance with ethical standards

**Conflict of interest** None.

## References

Barton M, Huijsmans JPP (1986) Post-caldera dacites from the Santorini volcanic complex, Aegean sea, Greece: an example of the eruption of lavas of near-constant composition over a 2,200 year period. Contrib Miner Petrol 94:472–495. https://doi.org/10.1007/BF00376340

Boudreau A (2016) Bubble migration in a compacting crystal-liquid mush. Contrib Miner Petrol 171(4):32. https://doi.org/10.1007/s00410-016-1237-9

Cashman KV (1993) Relationship between plagioclase crystallisation and cooling rate in basaltic melts. Contrib Miner Petrol 113:126–142. https://doi.org/10.1007/BF00320836

Cashman KV, Marsh BD (1988) Crystal size distribution (CSD) in rocks and the kinetics and dynamics of crystallisation II. Makaopuhi lava lake. Contrib Miner Petrol 99:292–305. https://doi.org/10.1007/BF00375363

Druitt TH, Edwards L, Mellors RM, Pyle D, Sparks RSJ, Lanphere M, Davies M, Barreirio B (1999a) Santorini volcano. In: Memoir vol. 19. Geological Society, London, p 176

Druitt TH, McCoy FW, Vougioukalakis GE (2019a) The Late Bronze Age eruption of Santorini volcano and Its impact on the ancient Mediterranean world. Elements 15(3):185–190. https://doi.org/10.2138/gselements.15.3.185

Druitt TH, Pyle DM, Mather TA (2019b) Santorini volcano and its plumbing system. Elements 15(3):177–184. https://doi.org/10.2138/gselements.15.3.177

Fornaciai A, Perinelli C, Armienti P, Favalli M (2015) Crystal size distributions of plagioclase in lavas from the July–August 2001 Mount Etna eruption. Bull Volcanol 77(8):1–15. https://doi.org/10.1007/s00445-015-0953-8

Francalanci L, Vougioukalakis G, Eleftheriadis G, Pinarelli L, Petrone C, Manetti P, Christofides G (1998) Petrographic, chemical and isotope variations in the intracaldera post-Minoan rocks of the Santorini volcanic field, Greece. In: Casale R (ed) Proceedings of the second workshop, Santorini, Greece, pp 175–186

Götze J, Schertl H-P, Neuser RD, Kempe U, Hanchar JM (2012) Optical microscope-cathodoluminescence (OM–CL) imaging as a powerful tool to reveal internal textures of minerals. Mineral Petrol 107(3):373–392. https://doi.org/10.1007/s00710-012-0256-0

Helz RT (1987) Differentiation behavior of Kilauea Iki lava lake, Kilauea Volcano, Hawaii; an overview of past and current work. Magmatic processes; physicochemical principles; a volume in honor of Hatten S Yoder, Jr, vol 1. Geochemical Society, Dayton, Ohio, pp 241–258

Higgins MD (1996a) Crystal size distributions and other quantitative textural measurements in lavas and tuff from Mt Taranaki (Egmont volcano), New Zealand. Bull Volcanol 58:194–204

Higgins MD (1996b) Magma dynamics beneath Kameni volcano, Thera, Greece, as revealed by crystal size and shape measurements. J Volcanol Geoth Res 70(1–2):37–48. https://doi.org/10.1016/0377-0273(95)00045-3

Higgins MD (2000) Measurement of crystal size distributions. Am Mineral 85(9):1105–1116. https://doi.org/10.2138/am-2000-8-901

Higgins MD (2006) Quantitative textural measurements in igneous and metamorphic petrology. Cambridge University Press, Cambridge, UK

Higgins MD (2010a) Imaging birefringent minerals without extinction using circularly polarized light. Can Mineral 48(1):231–235. https://doi.org/10.3749/canmin.48.1.231

Higgins MD (2010b) Textural coarsening in igneous rocks. Intern Geol Rev 53(3–4):354–376. https://doi.org/10.1080/00206814.2010.496177

Higgins MD, Voos S, Vander Auwera J (2015) Magmatic processes under Quizapu volcano, Chile, identified from geochemical and textural studies. Contrib Miner Petrol 170(5–6):1–16. https://doi.org/10.1007/s00410-015-1209-5

Hooft EEE, Heath BA, Toomey DR, Paulatto M, Papazachos CB, Nomikou P, Morgan JV, Warner MR (2019) Seismic imaging of Santorini: subsurface constraints on caldera collapse and present-day magma recharge. Earth Planet Sci Lett 514:48–61. https://doi.org/10.1016/j.epsl.2019.02.033

Huijsmans JPP (1985) Calc-alkaline lavas from the volcanic complex of Santorini, Aegean Sea, Greece: a petrological, geochemical and stratigraphic study. Geologica Ultraiectina 41:1–316

Le Maitre RW, Streckeisen A, Zanettin B, Le Bas MJ, Bonin B, Bateman P, Bellieni G, Dudek A, Efremova S, Keller J, Lameyre J, Sabine PA, Schmid R, Sorensen H, Woolley AR (2002) Igneous rocks : a classification and glossary of terms: recommendations of the International Union of Geological Sciences subcommission on the systematics of igneous rocks. Cambridge University Press, Cambridge

Marsh BD (1988) Crystal size distribution (CSD) in rocks and the kinetics and dynamics of crystallization I. Theory. Contrib Miner Pet 99:277–291. https://doi.org/10.1007/BF00375362

Martin VM (2005) Geochemical and textural analysis of mafic enclaves from Nea Kameni, Santorini, Greece. PhD Thesis, University of Cambridge

Martin VM, Holness MB, Pyle DM (2006) Textural analysis of magmatic enclaves from the Kameni Islands, Santorini, Greece. J Volcanol Geoth Res 154(1–2):89–102. https://doi.org/10.1016/j.jvolgeores.2005.09.021

Martin VM, Morgan DJ, Jerram DA, Caddick MJ, Prior DJ, Davidson JP (2008) Bang! month-scale eruption triggering at Santorini volcano. Science 321(5893):1178. https://doi.org/10.1126/science.1159584

McVey BG, Hooft EEE, Heath BA, Toomey DR, Paulatto M, Morgan JV, Nomikou P, Papazachos CB (2019) Magma accumulation beneath Santorini volcano, Greece, from P-wave tomography. Geology 48(3):231–235. https://doi.org/10.1130/g47127.1

Mills RD, Glazner AF (2013) Experimental study on the effects of temperature cycling on coarsening of plagioclase and olivine in an alkali basalt. Contrib Miner Petrol 166(1):97–111. https://doi.org/10.1007/s00410-013-0867-4

Mora CI, Ramseyer K (1992) Cathodoluminescence of coexisting plagioclases, boehls butte anorthosite-Cl activators and fluid-flow paths. Am Mineral 77(11–12):1258–1265

Mungall JE (2015) Physical Controls of Nucleation, Growth and Migration of Vapor Bubbles in Partially Molten Cumulates. In: Charlier B, Namur O, Latypov R, Tegner C (eds) Layered Intrusions. Springer, Dordrecht, pp 331–377

Newman AV, Stiros S, Feng L, Psimoulis S, Moschas S, Saltogianni V, Jiang Y, Papazachos C, Karaginni E, Vamvakaris D (2012) Recent geodetic unrest at Santorini Caldera, Greece. Geophys Res Lett. https://doi.org/10.1029/2012gl051286

Nicholls IA (1971) Petrology of Santorini Volcano, Cyclades. Greece J Petrol 12(1):67–119. https://doi.org/10.1093/petrology/12.1.67

Nomikou P, Parks MM, Papanikolaou D, Pyle DM, Mather TA, Carey S, Watts AB, Paulatto M, Kalnins ML, Livanos I, Bejelou K, Simou E, Perros I (2014) The emergence and growth of a submarine volcano: The Kameni islands, Santorini (Greece). GeoResJ 1-2(Supplement C):8-18 doi:https://doi.org/10.1016/j.grj.2014.02.002

Pagel M, Barbin V, Blanc P, Ohnenstetter D (2000) Cathodoluminescence in geosciences. Springer, Berlin

Parks MM, Biggs J, England P, Mather TA, Nomikou P, Palamartchouk K, Papanikolaou X, Paradissis D, Parsons B, Pyle DM, Raptakis C, Zacharis V (2012) Evolution of Santorini volcano dominated by episodic and rapid fluxes of melt from depth. Nat Geosci 5(10):749–754. https://doi.org/10.1038/ngeo1562

Parks MM, Moore JDP, Papanikolaou X, Biggs J, Mather TA, Pyle DM, Raptakis C, Paradissis D, Hooper A, Parsons B, Nomikou P (2015) From quiescence to unrest: 20 years of satellite geodetic measurements at Santorini volcano, Greece. J Geophys Res Solid Earth 120(2):1309–1328. https://doi.org/10.1002/2014JB011540

Petrone C, Francalanci L, Vougioukalakis G (2013) Mixing, mingling and enclave crumbling in the post-Minoan dacitic magmas of Santorini volcano, Greece. In: Goldschmidt 2013 conference proceedings

Pleše P, Higgins MD, Baker DR, Kudrna Prašek M (2019) Nucleation and growth of bubbles on plagioclase crystals during experimental decompression degassing of andesitic melts. J Volcanol Geoth Res 388:106679. https://doi.org/10.1016/j.jvolgeores.2019.106679

Pleše P, Higgins MD, Mancini L, Lanzafame G, Brun F, Fife JL, Casselman J, Baker DR (2018) Dynamic observations of vesiculation reveal the role of silicate crystals in bubble nucleation and growth in andesitic magmas. Lithos 296–299:532–546. https://doi.org/10.1016/j.lithos.2017.11.024

Pyle DM (2017) What Can We Learn from Records of Past Eruptions to Better Prepare for the Future? In: Fearnley CJ, Bird DK, Haynes K, McGuire WJ, Jolly G (eds) Observing the volcano world. Springer, Heidelberg, pp 1–18

Rasband WS (2010) ImageJ. U. S. National Institutes of Health, Bethesda, Maryland, USA http://rsb.info.nih.gov/ij/

Rizzo AL, Barberi F, Carapezza ML, Di Piazza A, Francalanci L, Sortino F, D'Alessandro W (2015) New mafic magma refilling a quiescent volcano: evidence from He-Ne-Ar isotopes during the 2011–2012 unrest at Santorini, Greece. Geochem Geophys Geosyst 16(3):798–814. https://doi.org/10.1002/2014gc005653

Ruprecht P, Simon AC, Fiege A (2020) The Survival of Mafic Magmatic Enclaves and the Timing of Magma Recharge. Geophysical Research Letters 47(14):e2020GL087186 doi:https://doi.org/https://doi.org/10.1029/2020GL087186

Sigurdsson H, Carey S, Alexandri M, Vougioukalakis G, Croff K, Roman C, Sakellariou D, Anagnostou C, Rousakis G, Ioakim C, Goguo A, Ballas D, Misaridis T, Nomikou P (2006) Marine investigations of Greece's Santorini volcanic field. Eos, Transactions American Geophysical Union 87(34):337–342. https://doi.org/10.1029/2006eo340001

Stamatelopoulou-Seymour K, Vlassopoulos D, Pearce TH, Rice C (1990) The record of magma chamber processes in plagioclase phenocrysts at Thera volcano, Aegean volcanic arc, Greece. Contrib Miner Petrol 104:73–84. https://doi.org/10.1007/BF00310647

Theodorakopoulou K, Kyriakopoulos K, Athanassas CD, Galanopoulos E, Economou G, Maniatis Y, Godelitsas A, Dotsika E, Mavridis F, Darlas A (2020) First Speleothem Evidence of the Hiera Eruption (197 BC), Santorini, Greece. Environmental Archaeology:1-13 doi:https://doi.org/10.1080/14614103.2020.1755196

Vougioukalakis GE, Fytikas M (2005) Volcanic hazards in the Aegean area, relative risk evaluation, monitoring and present state of the active volcanic centers. In: Fytikas M, Vougioukalakis GE (eds) The South Aegean active volcanic arc-present knowledge and future perspectives, milos conferences, vol 7. Elsevier, Greece, pp 161–183

Watts AB, Nomikou P, Moore JDP, Parks MM, Alexandri M (2015) Historical bathymetric charts and the evolution of Santorini submarine volcano. Greece Geochem Geophys Geosyst 16(3):847–869. https://doi.org/10.1002/2014gc005679

Zellmer G, Turner S, Hawkesworth C (2000) Timescales of destructive plate margin magmatism; new insights from Santorini, Aegean volcanic arc. Earth Planet Sci Lett 174(3–4):265–281. https://doi.org/10.1016/S0012-821X(99)00266-6

Zellmer GF, Blake S, Vance D, Hawkesworth C, Turner S (1999) Plagioclase residence times at two island arc volcanoes (Kameni Islands, Santorini, and Soufriere, St. Vincent) determined by Sr diffusion systematics. Contributions to Mineralogy and Petrology 136(4):345-357 doi:https://doi.org/10.1007/s004100050543